Magn Reson Med Sci 2021; 20; 431–438
doi:10.2463/mrms.mp.2020-0132 Published Online: February 2, 2021

MAJOR PAPER

Investigating the Image Quality and Utility of Synthetic MRI in the Breast

Tomoyuki Fujioka[1], Mio Mori[1*], Jun Oyama[1], Kazunori Kubota[1,2], Emi Yamaga[1], Yuka Yashima[1], Leona Katsuta[1], Kyoko Nomura[1], Miyako Nara[1,3], Goshi Oda[4], Tsuyoshi Nakagawa[4], and Ukihide Tateishi[1]

Purpose: Synthetic MRI reconstructs multiple sequences in a single acquisition. In the present study, we aimed to compare the image quality and utility of synthetic MRI with that of conventional MRI in the breast.

Methods: We retrospectively collected the imaging data of 37 women (mean age: 55.1 years; range: 20–78 years) who had undergone both synthetic and conventional MRI of T2-weighted, T1-weighted, and fat-suppressed (FS)-T2-weighted images. Two independent breast radiologists evaluated the overall image quality, anatomical sharpness, contrast between tissues, image homogeneity, and presence of artifacts of synthetic and conventional MRI on a 5-point scale (5 = *very good* to 1 = *very poor*). The interobserver agreement between the radiologists was evaluated using weighted kappa.

Results: For synthetic MRI, the acquisition time was 3 min 28 s. On the 5-point scale evaluation of overall image quality, although the scores of synthetic FS-T2-weighted images (4.01 ± 0.56) were lower than that of conventional images (4.95 ± 0.23; $P < 0.001$), the scores of synthetic T1- and T2-weighted images (4.95 ± 0.23 and 4.97 ± 0.16) were comparable with those of conventional images (4.92 ± 0.27 and 4.97 ± 0.16; $P = 0.484$ and 1.000, respectively). The kappa coefficient of conventional MRI was fair (0.53; $P < 0.001$), and that of conventional MRI was fair (0.46; $P < 0.001$).

Conclusion: The image quality of synthetic T1- and T2-weighted images was similar to that of conventional images and diagnostically acceptable, whereas the quality of synthetic T2-weighted FS images was inferior to conventional images. Although synthetic MRI images of the breast have the potential to provide efficient image diagnosis, further validation and improvement are required for clinical application.

Keywords: *breast, breast cancer, magnetic resonance imaging, synthetic magnetic resonance imaging*

Introduction

Breast cancer is the most common cancer and the second-leading cause of cancer-related deaths in women.[1] The diagnosis of breast images is conducted comprehensively using a plurality of modalities, such as mammography, ultrasound, MRI, and positron emission tomography.[2–5] MRI is widely used in routine practice for detecting and diagnosing breast tumor when an abnormality is found by other imagings and when screening high-risk patients or patients with a personal history of breast cancer.[6–8] Because dynamic contrast-enhanced (DCE) MRI is currently regarded as a very sensitive imaging tool for breast cancer detection, breast MRI examination mainly consists of DCE-MRI. T1-weighted, T2-weighted, and fat-suppressed (FS) images are some of the MRI sequences that are useful for detecting and estimating bleeding, fat, edema, and cyst.[9–14] However, because of limitations in total scan time for patients, some of these sequences may be omitted. In conventional MRI, the imaging parameters such as RT, TE, and inversion time (TI) are predetermined before the examination is conducted. Therefore, to obtain additional images

[1]Department of Diagnostic Radiology, Tokyo Medical and Dental University, Tokyo, Japan
[2]Department of Radiology, Dokkyo Medical University, Shimotsuga-gun, Tochigi, Japan
[3]Department of Breast Surgery, Tokyo Metropolitan Cancer and Infectious Diseases Center Komagome Hospital, Tokyo, Japan
[4]Department of Surgery, Breast Surgery, Tokyo Medical and Dental University, Tokyo, Japan
[*]Corresponding author: Department of Diagnostic Radiology, Tokyo Medical and Dental University, 1-5-45, Yushima, Bunkyo-ku, Tokyo 113–8510, Japan. Phone: +81-3-5803-5311, Fax: +81-3-5803-0147, Email: m_mori_116@yahoo.co.jp

Received: September 14, 2020 | Accepted: December 12, 2020

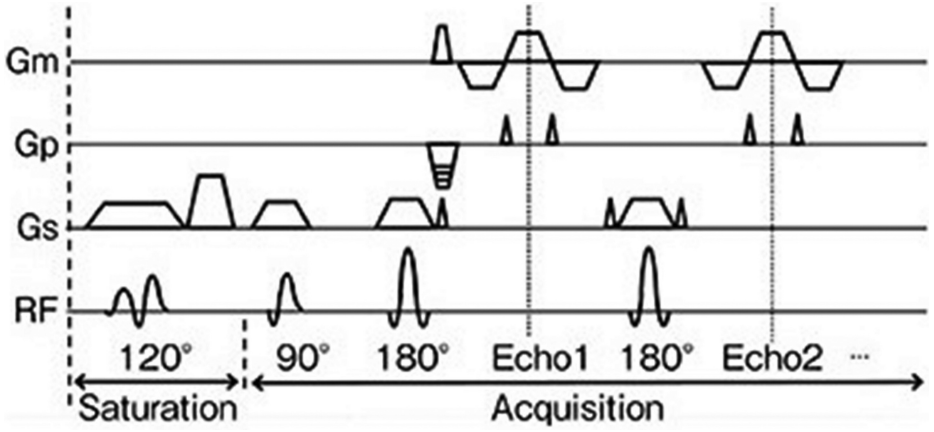

Fig. 1 Multidynamic multiecho sequence for synthetic MRI. The figure shows the Gm, Gp, and Gs and the RF pulse amplitude over time. There are two phases in each block. In first phase (saturation), the 120° saturation pulse and subsequent spoiling acts. In second phase (acquisition), the multi-echo spin-echo acquisition is performed, using the 90° excitation pulse and multiple 180° refocusing pulses. Gm, gradient in measurement; Gp, gradient in phase-encoding; Gs, gradient in slice-selection. This image is reprinted with permission from GE Healthcare Japan.

after the MRI examination, the patients must return to the hospital and undergo another MRI scanning.

Recently, a synthetic MRI technique has been developed and applied clinically. Synthetic MRI computes and uses quantitative values for multiple physical properties to reconstruct multiple contrasts from a single scan. Parameters such as TR, TE, and TI are not predetermined and can be changed arbitrarily by mathematical inference. This advance helps to reduce rescanning time and improve efficiency of examination.[15–17] The usefulness of synthetic MRI has been demonstrated primarily in the bone, joint, and central nervous system.[18–24] Several studies have reported that synthetic images have similar diagnostic utility to conventional image series, as well as good quality and contrast for lesion detection and characterization.

Little research has been conducted on synthetic MRI for breast images, and to our knowledge, there are no reports that have visually evaluated the image quality and clinical usefulness. Therefore, to enable the use of breast synthetic MRI in daily practice, a clinical study using actual patient data must be conducted. The present study aimed to compare the image quality and clinical usefulness of synthetic MRI with that of conventional MRI in the breast.

Materials and Methods

Study population

The Tokyo Medical and Dental University Hospital Ethics Committee approved this retrospective study (approval ID: M2019-137, approval date: September 19, 2019) and waived the requirement for written informed consent. The study was conducted according to the Declaration of Helsinki. Selection criteria for patient enrollment were as follows: (a) consecutive patients who underwent breast synthetic MRI at our hospital between February and May 2020, and (b) patients who were female and older than 20 years. After we examined the clinical records and database of radiology reports at our hospital, a breast radiologist with 10 years of consecutive experience extracted breast MRI data for the present study.

MRI protocol

With the patient in the prone position, MRI examinations were conducted using a 3.0-T MRI system (Signa Pioneer; GE Healthcare, Chicago, IL, USA) using a 16-channel phased-array bilateral breast coil (NeoCoil 3.0T 16-channel breast coil; GE Healthcare). Besides conventional MR sequences, all patients underwent a synthetic MR sequence. Synthetic MRI data were acquired using fast spin-echo multidynamic multiecho sequence (MAGiC [magnetic resonance image compilation]; GE Healthcare). The synthetic MR sequence included four automatically calculated saturation delays and two TRs (Fig. 1).[17] To quantify the properties of physical tissue, such as longitudinal T1, transverse T2 relaxation times, and proton density (PD), each acquisition produced eight real images and eight imaginary images per section using various combinations of saturation delay and TR (Figs. 2 and 3). Synthetic T1- and T2-weighted images, as well as short tau inversion recovery (STIR) images, were generated from the raw data produced by synthetic imaging sequence using a vendor-provided program (SyMRI; SyntheticMR, Linköping, Sweden) with TR, TE, and TI. In the present study, STIR images of synthetic MRI were defined as FS-T2-weighted images. Conventional T1-, T2-, and FS-T2-weighted images were obtained based on the standard imaging protocol of our institution. We used

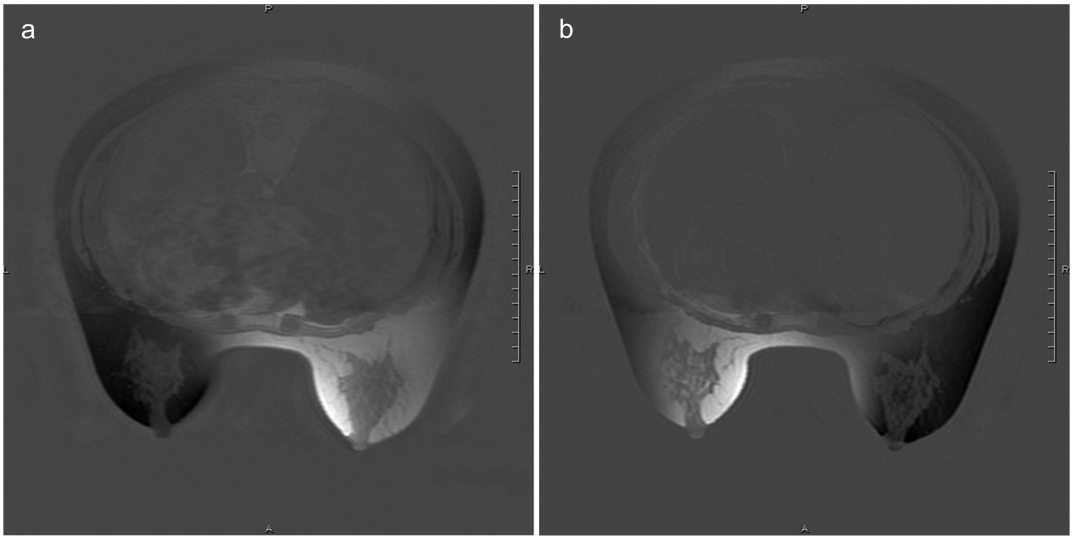

Fig. 2 Real image and imaginary image. Using different combinations of echo time and saturation delay, each acquisition produced (**a**) real images and (**b**) imaginary images per section for the quantification of the physical properties of tissue.

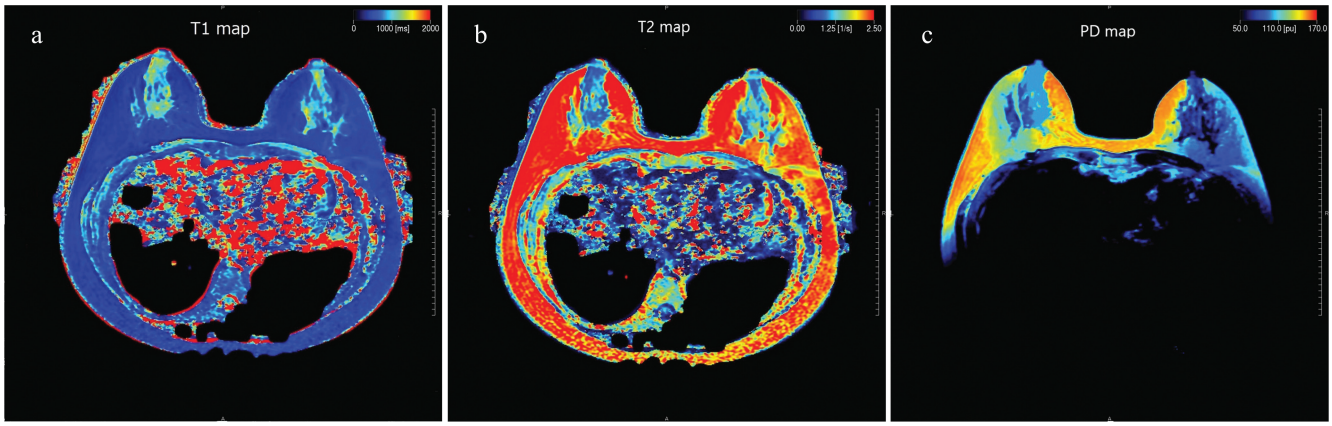

Fig. 3 T1, T2, and PD maps. Quantitative images of (**a**) T1, (**b**) T2, and (**c**) PD maps were generated by quantification of the physical properties of tissue. PD, proton density.

gradient echo sequence to acquire T1-weighted images. T2-weighted images were acquired using fast spin-echo sequence, and FS of conventional MRI was conducted using the two-point DIXON sequence (FLEX; GE Healthcare). The detailed parameters of the MR sequences are shown in Table 1.

Image analysis

In the present study, two radiologists (reader 1 with 6 years of experience and reader 2 with 10 years of experience in breast imaging) independently evaluated the breast MRIs with knowledge of the patient's age and clinical course. They simultaneously read each patient's synthetic and conventional T1-, T2-, and FS-T2-weighted MRIs and conducted a visual evaluation of the overall image quality, anatomical sharpness, tissues contrast, image homogeneity, and status of artifacts of the images using a 5-point scale evaluation (5 = *very good*, 4 = *good*, 3 = *acceptable*, 2 = *poor*, and 1 = *very poor*). The readers evaluated the images knowing whether they were synthetic or conventional images. In the present study, anatomical sharpness was defined as the sharpness of the anatomical structures between the mammary gland, fat, and tumor; tissue contrast as the clarity of the contrast between those tissues; image homogeneity as the stability of the image with less signal unevenness and graininess; and status of artifacts as a motion artifact due to body movement or heartbeat. We used the medical viewing system EV Insite R (PSP, Tokyo, Japan), which provides reading tools, such as window width–window level adaptation, panning, and zooming.

Table 1 MRI acquisition parameters.

Sequence	Sy T1-WI	Sy T2-WI	Sy FS-T2-WI	T1-WI	T2-WI	FS-T2-WI[b]
TR (ms)	500	5000	15000	5.4	3000	3000
TE (ms)	10	85	100	2.6	85	85
TI (ms)	—	—	260	—	—	—
Flip angle (°)	—	—	—	10	—	—
Field of view (mm)	360	360	360	360	360	360
Section thickness (mm)	4	4	4	2(4)[a]	4	4
Intersection gap (mm)	4	4	4	2(4)[a]	4	4
Bandwidth (Hz/pixel)	462.9	462.9	462.9	559	125	125
Echo-train length	16	16	16	—	14	14
Acceleration factor	2	2	2	2.25	2	2
Acquisition time (min:s)	3:28	3:28	3:28	0:43	2:21	2:21

T1-WI were acquired with a section thickness of 2 mm and an intersection gap of 2 mm and reconstructed into a section thickness of 4 mm and an intersection gap of 4 mm. FS was conducted using the two-point DIXON sequence. FS, fat-suppressed; Sy, synthetic; WI, weighted images.

Statistical analysis

We present the results as means ± standard deviations (SDs). All statistical analyses were conducted using the software SPSS for Windows (version 24.0; IBM, Armonk, NY, USA). We conducted a Wilcoxon signed-rank test to compare the 5-point scale evaluations of the T1-, T2-, and FS-T2-WI between the synthetic and conventional MRI.

We evaluated interobserver agreement using weighted kappa. Kappa coefficient was calculated by comparing the 5-point scale evaluation scores of the two readers and interpreted as follows: < 0.20, slight; 0.21–0.40, fair; 0.41–0.60, moderate; 0.61–0.80, substantial; and 0.81–1.0, almost perfect.[25] We considered a P-value of < 0.05 to be statistically significant.

Results

Thirty-seven patients were included in the present study. The patients' age ranged from 20 to 78 years (mean ± SD; 55.1 ± 14.2 years). The purposes of the MRI were staging before treatment planning (n = 16), problem-solving for abnormalities found in mammography or ultrasonography (n = 17), post-operative follow-up (n = 3), and screening of high-risk patients (n = 1). Twenty-four patients were diagnosed with breast cancer and 13 patients were diagnosed as benign or normal.

The comparison of scores for synthetic MRI and conventional MRI is shown in Table 2. For T1- and T2-WI, both readers 1 and 2 scored all evaluation items of both synthetic and conventional MRI as 4 or 5. For FS-T2-WI, although the readers scored all items of conventional MRI and tissue contrast of synthetic MRI as 4 or 5, they scored overall image quality, anatomical sharpness, image homogeneity, and the status of artifacts as 3, 4, or 5.

There were no significant differences between the synthetic and conventional MRI in all evaluation items in T1-WI. However, in T2-WI, reader 1 scored image homogeneity and the status of artifacts significantly higher in conventional MRI, whereas reader 2 scored tissue contrast significantly higher in synthetic MRI. Although there was no significant difference in tissue contrast in T2-FS-WI, both readers 1 and 2 scored overall image quality, anatomical sharpness, image homogeneity, and status of artifacts significantly higher in conventional MRI than in synthetic MRI.

The average kappa coefficient between the two radiologists for evaluating image quality was 0.53 (range, 0.52–0.56; $P < 0.001$) for conventional MRI and 0.46 (range, 0.37–0.57; $P < 0.001$) for synthetic MRI (Table 3).

Representative cases of synthetic MRI and conventional MRI in the breast are displayed in Fig. 4.

Discussion

Simultaneous relaxometry techniques, which map the relaxation parameters of tissues, are state-of-the-art imaging technologies that have attracted attention for the expectation that they will eliminate the need for rescans and increase the efficiency of the examination. Presently, two major simultaneous relaxation measurements are used: synthetic MRI and MR fingerprinting (MRF).[15] Synthetic MRI maps T1 and T2 relaxation times and PD, and generates multiple images of various conditions, such as T1- and T2-WI, fluid-attenuated inversion recovery (FLAIR) images, and STIR images, with a single acquisition.[16,17] MRF is another innovative method for the simultaneous quantification of tissue characteristics. The basic process of MRI acquires data in a pseudorandom manner and generates unique patterns of signal evolution unique to each tissue. These unique signals are then matched

Table 2 Comparison of scores for synthetic MRI and conventional MRI

	Reader 1		*P*	Reader 2		*P*
	T1-WI	Sy T1-WI		T1-WI	Sy T1-WI	
Overall image quality	4.97 ± 0.16	4.95 ± 0.23	0.773	4.86 ± 0.35	4.95 ± 0.23	0.149
Anatomical sharpness	5.00 ± 0.00	4.95 ± 0.23	0.346	4.92 ± 0.28	4.89 ± 0.31	0.777
Contrast between tissues	4.97 ± 0.16	5.00 ± 0.00	1.000	4.92 ± 0.28	4.84 ± 0.37	0.233
Image homogeneity	4.86 ± 0.42	4.86 ± 0.35	0.351	4.78 ± 0.42	4.73 ± 0.45	0.530
Presence of artifacts	4.57 ± 0.50	4.49 ± 0.51	0.299	4.62 ± 0.49	4.73 ± 0.45	0.267
	T2-WI	Sy T2-WI		T2-WI	Sy T2-WI	
Overall image quality	5.00 ± 0.00	4.97 ± 0.16	1.000	4.95 ± 0.23	4.97 ± 0.16	0.773
Anatomical sharpness	5.00 ± 0.00	4.97 ± 0.16	1.000	4.81 ± 0.40	4.95 ± 0.23	0.073
Contrast between tissues	5.00 ± 0.00	5.00 ± 0.00	1.000	4.62 ± 0.49	4.97 ± 0.16	0.001
Image homogeneity	5.00 ± 0.00	4.81 ± 0.40	0.011	4.95 ± 0.23	4.81 ± 0.40	0.110
Presence of artifacts	4.95 ± 0.23	4.78 ± 0.42	0.020	4.95 ± 0.23	4.86 ± 0.35	0.299
	FS-T2-WI	Sy FS-T2-WI		FS T2-WI	Sy FS-T2-WI	
Overall image quality	4.97 ± 0.16	3.81 ± 0.40	0.000	4.92 0.28	4.22 ± 0.63	0.000
Anatomical sharpness	4.97 ± 0.16	4.16 ± 0.76	0.000	4.81 0.40	4.41 ± 0.50	0.000
Contrast between tissues	5.00 ± 0.00	4.89 ± 0.39	0.174	4.89 0.31	4.76 ± 0.86	0.608
Image homogeneity	5.00 ± 0.00	3.51 ± 0.51	0.000	4.81 0.40	4.00 ± 0.53	0.000
Presence of artifacts	4.68 ± 0.47	3.97 ± 0.29	0.000	4.81 0.40	4.35 ± 0.48	0.000

Values represent means ± standard deviation. Wilcoxon's signed-rank test was conducted. FS, fat-suppressed; Sy, synthetic; WI, weighted images.

Table 3 Weighted kappa for evaluating image quality between the two readers

	Conventional MRI		Synthetic MRI	
	Kappa coefficient (95% CI)	*P*	Kappa coefficient (95% CI)	*P*
T1-WI	0.56 (0.39–0.73)	< 0.001	0.52 (0.35–0.70)	< 0.001
T2-WI	0.52 (0.34–0.69)	< 0.001	0.57 (0.39–0.74)	< 0.001
FS-T2-WI	0.52 (0.35–0.69)	< 0.001	0.37 (0.21–0.53)	< 0.001
Average	0.53		0.46	

CI, confidence interval; FS, fat-suppressed; WI, weighted images.

to a predefined dictionary of signal fingerprints, and quantitative maps of T1, T2, and PD are generated.[26]

Although there have been several reports of synthetic MRI (primarily in neuroimaging) and its usefulness has been proven, there is little evidence of the use of synthetic MRI in breast imaging. The present study verified the image quality and clinical utility of synthetic MRI by comparing it with conventional MRI of T1-, T2-, and FS-T2-WI in the breast.

T1- and T2-weighted synthetic MRI had high values on the 5-point scale evaluations, and the image quality was almost the same as that of conventional images. Therefore, we propose that these synthetic images can be applied to clinical practice. However, although FS-T2-WI of synthetic MRI demonstrated a contrast that was similar to that of conventional images, synthetic images were inferior to conventional images in other evaluation items. To enable practical use of FS-T2-WI of synthetic MRI, it is necessary to fully understand not only the advantages but also the disadvantages of the images. In the present study, we demonstrated a fair concordance rate between two readers on synthetic MRI, which supports the fact that synthetic MRI is both reproducible and stable. In general, synthetic MRI has

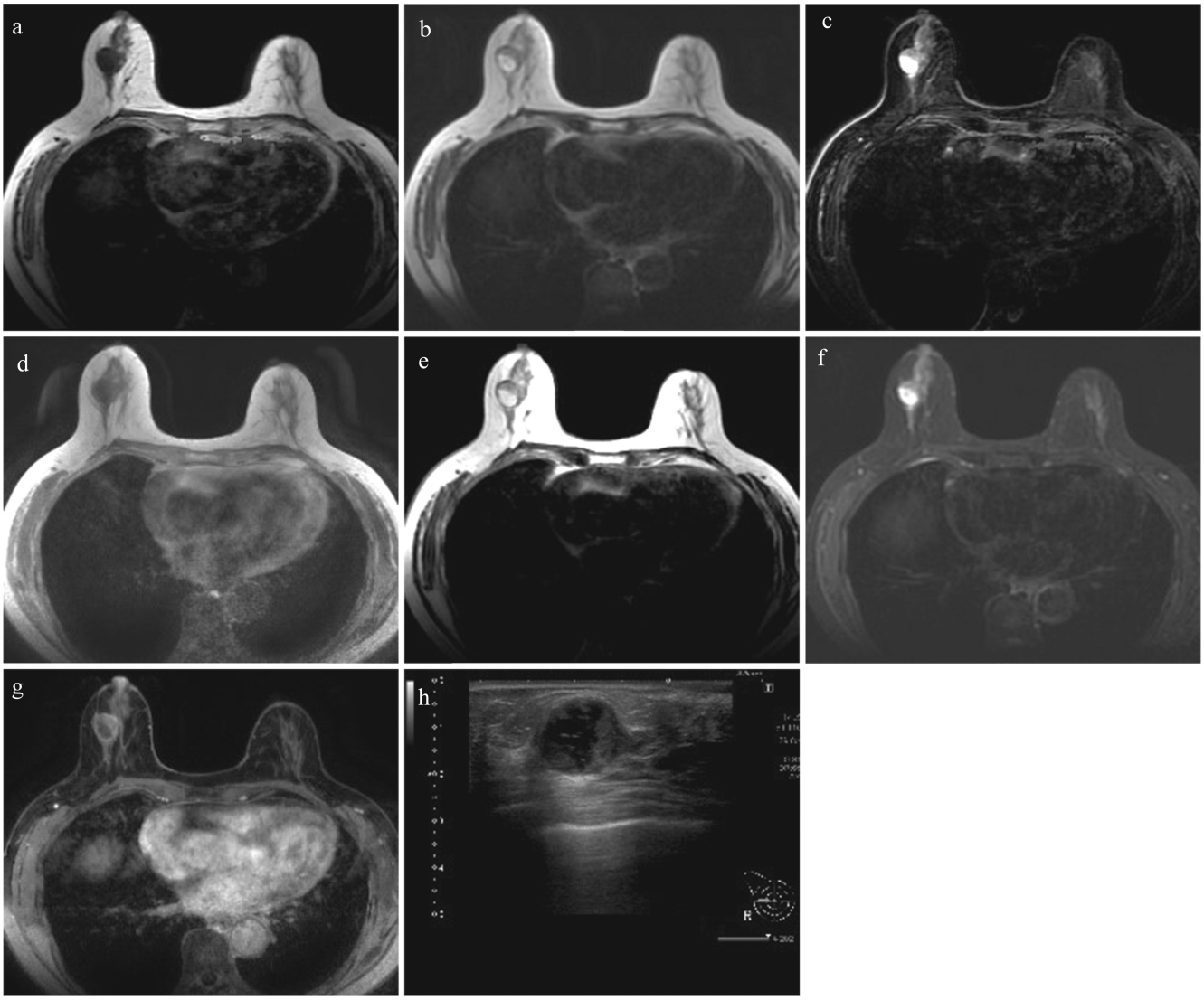

Fig. 4 Case 1 of Sy MRI and conventional MRI in the breast. A 69 year-old woman with noninfiltrating intracystic carcinoma (18 mm) in the right breast. Sy MRI (**a**–**c**) and conventional MRI (**d**–**f**) clearly show solid component as low signal intensity of the T1-WI and iso-signal intensity of T2- and FS-T2-WI and cystic components as low signal intensity of T1-WI and high signal intensity of T2- and FS-T2-WI. Contrast-enhanced T1-WI (**g**) and ultrasound image (**h**) show a mass composed of solid and cystic components. Sy T1-WI (**a**), Sy T2-WI (**b**), Sy FS-T2-WI (**c**), T1-WI (**d**), T2-WI (**e**), FS-T2-WI (**f**), contrast-enhanced T1-WI (**g**), and ultrasound image (**h**). FS, fat-suppressed; Sy, synthetic; T1-WI, T1-weighted image; T2-WI, T2-weighted image.

a potential to synthesize multiple sequences of images in a shorter time compared to the conventional scan. Another promising application may be to synthesize contrast-enhanced image from non-enhanced image, which can be especially useful for patients who should not use contrast agents due to a history of allergies or asthma, for patients who are pregnant, and for patients who have difficulty staying in the MRI machine for long periods of time.

Several reports have examined the use of synthetic MRI for neuroimaging. In much of that research, synthetic and conventional MRIs were shown to have similar image quality for T1- and T2-weighted imaging. However, researchers have reported that in FLAIR images using the IR sequence, the image quality of synthetic MRI was inferior to that of conventional MRI.[19,21] These results suggest that synthetic MRI is unsuitable for images of IR sequence such as STIR and FLAIR images. Because it is difficult to suppress the fat signal of the entire breast homogeneously, the quality of FS synthetic MRI is considered to be deteriorated. The volume and shape of the breast vary from person to person, and adding appropriate fat suppression to the breast is more challenging than neuroimaging. Further

improvements might be required to generate images of IR sequences with synthetic MRI in the breast.

Artificial intelligence, especially deep learning technology, has recently attracted attention because of its outstanding performance in medical image processing. One of the most interesting breakthroughs in this area is the invention of generative adversarial networks (GANs).[27–29] GANs are a special type of neural network, one focusing on image generation and the other on discrimination. GAN has been reported to have broad applicability in medical imaging for image synthesis. Mori et al. aimed to generate and evaluate synthetic MRI of FS-T1-weighted imaging using pix2pix, which is one of the GANs used for image-to-image translation.[30] They demonstrated that, using this technique, realistic FS-T1-WI can be generated from T1-WI. We expect that research on image synthesis using the deep learning method will also progress in the future.

Although we focused only on the image quality of synthetic MRI in the present study, it is known that T1-, T2-, and FS-T2-WI are useful in the estimation of tissue components such as bleeding, fat, cysts, and edema. Several prior studies have reported no significant difference in diagnostic accuracy between synthetic and conventional images in neuroimaging. Thus, verification is needed to determine whether the image findings of synthetic MRI correlate with these tissue components and can contribute to the differential diagnosis of benign or malignant, as in conventional imaging for breast lesions.

Although we conducted only visual qualitative evaluation in the present study, it is possible to extract quantitative values such as T1, T2, and PD values using synthetic MRI. Jung et al. compared the T2 relaxation times acquired from synthetic MRI to that of multi-echo spin-echo (MESE) sequences and evaluated the clinical usefulness of synthetic MRI.[31] The mean T2 relaxation times of breast cancer were 84.75 ms by synthetic MRI and 90.35 ms by MESE T2 mapping, and those of fat tissue were 129.22 and 102.11 ms, respectively. Jung et al. indicated that there was a significant positive correlation between synthetic MRI and MESE sequences for breast cancer and for fat tissue.[31] Matsuda et al. examined the value of synthetic MRI in predicting the Ki-67 status in patients with estrogen receptor-positive breast cancer.[32] They reported that the SD of T1 TR of the contrast-enhanced image was significantly greater in the high-proliferation group than in the low-proliferation group and was a significant and independent predictor of Ki-67 expression.[32] Additional studies are needed and expected to elucidate whether the quantitative value by synthetic MRI is different for benign and malignant tumors and whether this value is associated with tumor grade and patient prognosis. If the usefulness of these quantitative evaluations by synthetic MRI is proved, synthetic MRI will make a great contribution to the diagnosis and treatment of breast cancer.

This study has several limitations. First, this was a retrospective study conducted at a single institution and included a relatively small number of cases. Therefore, prospective large-scale, multicenter studies are required to confirm the findings of this research. Second, in the present study, the values of TE, TR, and IR for synthetic MRI were set to predetermined values. By using a dedicated workstation for synthetic MRI, a reader can finely adjust TE, TR, and IR in the same way as window values are adjusted on computed tomography images. Further verification is needed to determine the suitable values of TE, TR, and IR for synthetic MRI. Third, for the FS sequence for FS-T2-WI, the IR method was used for synthetic MRI, and the DIXON method was used for conventional MRI. These differences in FS methods could have affected the evaluation of image quality.

Conclusion

The image quality of synthetic T1- and T2-WI was similar to that of conventional images and was diagnostically acceptable, whereas the quality of synthetic T2-weighted FS images was inferior to that of conventional images. Although synthetic MRI images of the breast have the potential to provide efficient image diagnosis, further validation and improvement are necessary for clinical application.

Acknowledgment

The authors would like to thank Enago (www.enago.jp) for the English language review.

Conflicts of Interest

The authors declare no conflict of interest.

References

1. Siegel RL, Miller KD, Jemal A. Cancer statistics, 2018. CA Cancer J Clin 2018; 68:7–30.
2. Fiorica JV. Breast cancer screening, mammography, and other modalities. Clin Obstet Gynecol 2016; 59:688–709.
3. Kornecki A. Current status of breast ultrasound. Can Assoc Radiol J 2011; 62:31–40.
4. Fujioka T, Kubota K, Kikuchi Y, et al. The feasibility of using 18F-FDG-PET/CT in patients with mucinous breast carcinoma. Nucl Med Commun 2018; 39:1033–1038.
5. Fujioka T, Kubota K, Toriihara A, et al. Tumor characteristics of ductal carcinoma in situ of breast visualized on [F-18] fluorodeoxyglucose-positron emission tomography/computed tomography: Results from a retrospective study. World J Radiol 2016; 8:743–749.
6. Sippo DA, Burk KS, Mercaldo SF, et al. Performance of screening breast MRI across women with different elevated breast cancer risk indications. Radiol 2019; 292:51–59.
7. Shimauchi A, Machida Y, Maeda I, et al. Breast MRI as a Problem-solving study in the evaluation of BI-RADS categories 3 and 4 microcalcifications: Is it worth performing? Acad Radiol 2018; 25:288–296.

8. Mann RM, Cho N, Moy L. Breast MRI: State of the art. Radiol 2019; 292:520–536.
9. Chau AC, Hua J, Taylor DB. Analysing breast tissue composition with MRI using currently available short, simple sequences. Clin Radiol 2016; 71:287–292.
10. Santamaría G, Velasco M, Bargalló X, et al. Radiologic and pathologic findings in breast tumors with high signal intensity on T2-weighted MR images. Radiographics 2010; 30:533–548.
11. Westra C, Dialani V, Mehta TS, et al. Using T2-weighted sequences to more accurately characterize breast masses seen on MRI. AJR Am J Roentgenol 2014; 202:183–190.
12. Durur-Subasi I, Durur-Karakaya A, Alper F, et al. Breast lesions with high signal intensity on T1-weighted MR images. Jpn J Radiol 2013; 31:653–661.
13. Harada TL, Uematsu T, Nakashima K, et al. Is the presence of edema and necrosis on T2WI pretreatment breast MRI the key to predict pCR of triple negative breast cancer? Eur Radiol 2020; 30:3363–3370.
14. Nakashima K, Uematsu T, Sugino T, et al. T2-hypointense rim of breast mass lesions on magnetic resonance images: Radiologic-pathologic correlation. Breast J 2018; 24:944–950.
15. Fujita S, Hagiwara A, Aoki S, et al. Synthetic MRI and MR fingerprinting in routine neuroimaging protocol: What's the next step? J Neuroradiol 2020; 47:134–135.
16. Andica C, Hagiwara A, Hori M, et al. Review of synthetic MRI in pediatric brains: Basic principle of MR quantification, its features, clinical applications, and limitations. J Neuroradiol 2019; 46:268–275.
17. Warntjes JB, Leinhard OD, West J, et al. Rapid magnetic resonance quantification on the brain: Optimization for clinical usage. Magn Reson Med 2008; 60:320–329.
18. Granberg T, Uppman M, Hashim F, et al. Clinical Feasibility of Synthetic MRI in Multiple Sclerosis: A Diagnostic and Volumetric Validation Study. AJNR Am J Neuroradiol 2016; 37:1023–1029.
19. Ryu KH, Baek HJ, Moon JI, et al. Initial clinical experience of synthetic MRI as a routine neuroimaging protocol in daily practice: A single-center study. J Neuroradiol 2020; 47:151–160.
20. Hagiwara A, Hori M, Yokoyama K, et al. Synthetic MRI in the detection of multiple sclerosis plaques. AJNR Am J Neuroradiol 2017; 38:257–263.
21. Lee SM, Choi YH, Cheon JE, et al. Image quality at synthetic brain magnetic resonance imaging in children. Pediatr Radiol 2017; 47:1638–1647.
22. Yi J, Lee YH, Song HT, et al. Clinical feasibility of synthetic magnetic resonance imaging in the diagnosis of internal derangements of the knee. Korean J Radiol 2018; 19:311–319.
23. Kumar NM, Fritz B, Stern SE, et al. Synthetic MRI of the knee: Phantom validation and comparison with conventional MRI. Radiol 2018; 289:465–477.
24. Boudabbous S, Neroladaki A, Bagetakos I, et al. Feasibility of synthetic MRI in knee imaging in routine practice. Acta Radiol Open 2018; 7:2058460118769686.
25. Landis JR, Koch GG. The measurement of observer agreement for categorical data. Biometrics 1977; 33:159–174.
26. Ma D, Gulani V, Seiberlich N, et al. Magnetic resonance fingerprinting. Nat 2013; 495:187–192.
27. Fujioka T, Mori M, Kubota K, et al. Breast ultrasound image synthesis using deep convolutional generative adversarial networks. Diagnostics (Basel) 2019; 9:176.
28. Fujioka T, Kubota K, Mori M, et al. Virtual interpolation images of tumor development and growth on breast ultrasound image synthesis with deep convolutional generative adversarial networks. J Ultrasound Med 2021; 40:61–69.
29. Fujioka T, Kubota K, Mori M, et al. Efficient anomaly detection with generative adversarial network for breast ultrasound imaging. Diagnostics (Basel) 2020; 10:456.
30. Mori M, Fujioka T, Katsuta L, et al. Feasibility of new fat suppression for breast MRI using pix2pix. Jpn J Radiol 2020; 38:1075–1081.
31. Jung Y, Gho SM, Back SN, et al. The feasibility of synthetic MRI in breast cancer patients: Comparison of T2 relaxation time with multiecho spin echo T2 mapping method. Br J Radiol 2018; 92:20180479.
32. Matsuda M, Kido T, Tsuda T, et al. Utility of synthetic MRI in predicting the Ki-67 status of oestrogen receptor-positive breast cancer: A feasibility study. Clin Radiol 2020; 75:398.e1-398.e8.